Star Formation Main Sequence in a Hierarchical Universe

ChangHoon Hahn[1,2], Jeremy L. Tinker[2], Andrew R. Wetzel[3,4,5]

changhoon.hahn@lbl.gov

DRAFT --- 4e8abfb --- 2018-08-06 --- NOT READY FOR DISTRIBUTION

ABSTRACT

motivation, methodology, impact. In observations star forming galaxies form a tight $log\ M_*$ to $log\ SFR$ relation referred to as the *star formation main sequence* (SFMS) out to $z \sim 2$. Beyond the evolution "along" this SFMS, however, the star formation histories of star forming galaxies have not been precisely characterized. The SFH of these galaxies govern SMF, SFMS, and also observed constraints on the stellar mass to halo mass relation.

By combining high-resolution cosmological N-body simulation with observed evolutionary trends of SF galaxies, we construct a model that tracks the evolution of star forming central galaxies over the redshift $z < 1$. Comparing this model

Observations find a remarkably small scatter in the stellar mass to halo mass relation. Somehow the star formation histories of galaxies must

According to observations, star forming galaxies form a tight $log\ M_*$ to $log\ SFR$ relation referred to as the "star formation main sequence" out to $z \sim 2$.

Subject headings: methods: numerical – galaxies: clusters: general – galaxies: groups: general – galaxies: evolution – galaxies: haloes – galaxies: star formation – cosmology: observations.

1. Introduction

- Motivate why we think SF galaxies evolve along the main sequence

- Discuss the current thought process on galaxy assembly bias

- Explain the limitation of SFH derivable from observations (Claire's fisher matrix paper would be really good; ask her about the details)

[1]Lawrence Berkeley National Laboratory, 1 Cyclotron Road, Berkeley, CA 94720

[2]Center for Cosmology and Particle Physics, Department of Physics, New York University, 4 Washington Place, New York, NY 10003

[3]TAPIR, California Institute of Technology, Pasadena, CA USA

[4]Carnegie Observatories, Pasadena, CA USA

[5]Department of Physics, University of California, Davis, CA USA

- Observations also can't provide detail host dark matter halo properties

- So the approach with combining observations with N-body (empirical modeling) is very effective in the context of the halo.

- Maybe talk about how the bigger context of why this is important?

- Why only centrals – because our current best understanding of satellites is that they quench after infall, so it doesn't make sense to look at them

- our model goes from $z < 1$ because beyond that the observations are statistically meaningless.

2. Central Galaxies of SDSS DR7

We construct our galaxy sample following the sample selection of Tinker et al. (2011). We select a volume-limited sample of galaxies with $M_r 5log(h) < 18$ and complete in $M_* > 10^{9.4} M_\odot$ from the NYU Value-Added Galaxy Catalog (VAGC; Blanton et al. 2005) of the Sloan Digital Sky Survey Data Release 7 (SDSS DR7; Abazajian et al. 2009) at $z \approx 0.04$. The stellar masses of these galaxies are estimated using the kcorrect code (Blanton & Roweis 2007) assuming a Chabrier (2003) initial mass function. The star formation of the galaxies are estimated spectroscopically using the specific star formation rates (SSFR) from the current release of the MPA-JHU spectral reductions[1] (Brinchmann et al. 2004). Generally speaking, $SSFR > 10^{-11} yr^{-1}$ are derived from H_α emission, $10^{-11} > SSFR > 10^{-12} yr^{-1}$ are derived from a combination of emission lines, and $SSFR < 10^{-12} yr^{-1}$ are based on $D_n 4000$ (see discussion in Wetzel et al. 2013). We note that $SSFR < 10^{-12} yr^{-1}$ should only be considered upper limits to the true galaxy SSFR (Salim et al. 2007).

From our galaxy sample, we identify the central galaxies using the Tinker et al. (2011) halo-based group-finding algorithm, which is based on the Yang et al. (2005) algorithm and tested in Campbell et al. (2015). The algorithm assigns a probability of being a satellite, P_{sat}, to each galaxy in the sample. Galaxies with $P_{sat} \geq 0.5$ are classified as satellites and $P_{sat} < 0.5$ are classified as centrals. In this paper we focus on central galaxies. With any group finding algorithm, galaxies are misassigned due to projection effects and redshift space distortions. The purity of the full central galaxy sample is $\sim 90\%$ with a completeness of $\sim 95\%$ (Tinker et al. 2017). Furthermore, Campbell et al. (2015) find that the algorithm robustly identifies red and blue centrals as a function of stellar mass, which is highly relevant to our analysis.

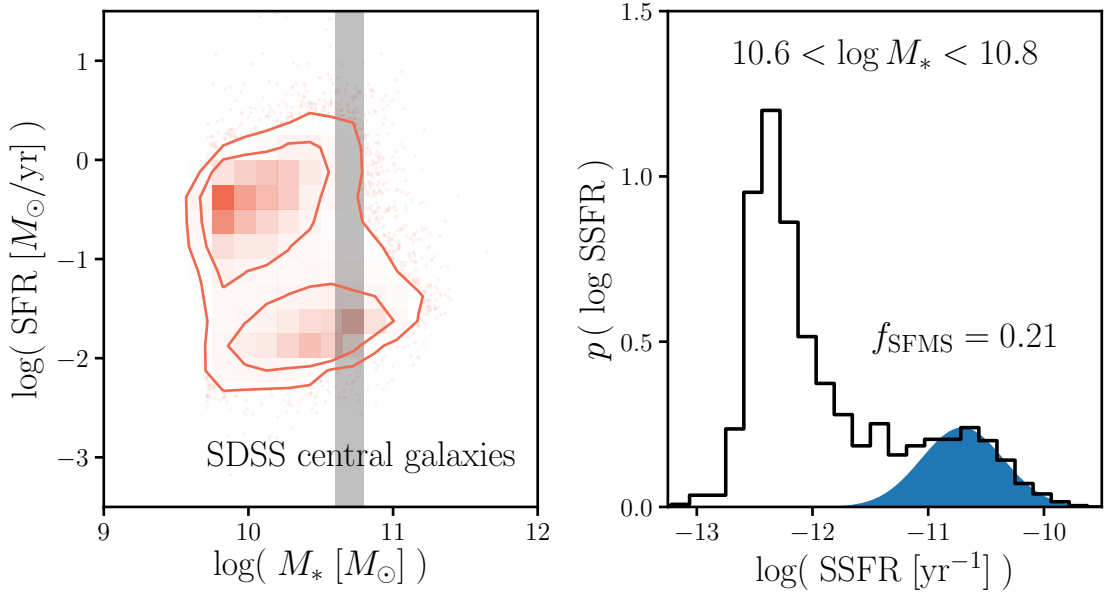---

[1]http://wwwmpa.mpa-garching.mpg.de/SDSS/DR7/

Fig. 1.— Central galaxies of the SDSS DR7 group catalog. *Left:* We plot the SFR-M_* relation of the SDSS central galaxies. The contours illustrate the bimodal distribution of the galaxy properties and mark the star-forming and quiescent populations. The transitioning galaxies lie on the "green" valley between the star-fomring and quiescent modes. *Right:* We plot the distribution of $\log$ SSFR for SDSS centrals with $10.6 < \log M_* < 10.8$. Shaded in blue, we plot the SFMS component of our GMM fit of the SFR-M_* relation described in Section 3.1. Based on this fit, galaxies in the SFMS account for approximately $f_{\rm SFMS} = 0.21$ of the central galaxies in the stellar mass bin.

In the left panel of Figure 1, we plot the SFR-M_* distribution of the SDSS DR7 central galaxies. In the right panel, we plot the distribution of SSFR, $p(\log \text{SSFR})$, for galaxies with $10.6 < \log M_* < 10.8$ (stellar mass range highlighted on the left panel). Both panels of Figure 1 illustrate the bimodality in the galaxy sample. The SFR-M_* distribution also illustrate the correlation between SFR and M_* in star-forming galaxies *i.e.* the star-formation main sequence (SFMS).

3. Model: Simulated Central Galaxies

We're interesting in constructing a model that tracks central galaxies and their star formation within the heirarchical growth of their host halos. This requires a cosmological N-body simulation that accounts for the complex dynamical processes that govern the host halos of galaxies. In this paper we use the high resolution N-body simulation from Wetzel et al. (2013) generated using the White (2002) `TreePM` code with flat ΛCDM cosmology ($\Omega_m = 0.274, \Omega_b = 0.0457, h = 0.7, n = 0.95, \text{and} \sigma_8 = 0.8$). From initial conditions at $z = 150$ generated from second-order Lagrangian Perturbation Theory, 2048^3 particles with mass of $1.98 \times 10^8 \, M_\odot$ are evolved in a $250\text{Mpc}/h$ box with a Plummer equivalent smoothing of $2.5 \, \text{kpc}/h$. For a more detailed description of the simulation, we refer readers to Wetzel et al. (2013, 2014).

From the TreePM N-body simulation, 'host halos' are identified using the Friends-of-Friends (FoF) algorithm of Davis et al. (1985) with linking length of $b = 0.168$ times the mean inter-partcile spacing. Within these host halos, Wetzel et al. (2013) identifies 'subhalos' as overdensities in phase space through a six-dimensional FoF algorithm (FoF6D White et al. 2010). The host halos and subhalos are then tracked across the 45 simulation outputs from $z = 10$ to 0 to build merger trees (Wetzel et al. 2009; Wetzel & White 2010). The most massive subhalos in newly-formed host halos at a given simulation output are defined as the 'central' subhalo. A central subhalo retains its 'central' definition until it falls into a more massive host halo, at which point it becomes a 'satellite' subhalo.

Each subhalo is assigned a M_{peak}, the maxmum host halo mass that it ever had as a central subhalo. Using M_{peak}, we construct a galaxy catalog from the subhalos using subhalo abundance matching (SHAM; Conroy et al. 2006; Vale & Ostriker 2006; Yang et al. 2009; Wetzel et al. 2012; Leja et al. 2013; Wetzel et al. 2013, 2014; Hahn et al. 2017a). In principle, SHAM assumes a one-to-one mapping between subhalo M_{peak} and galaxy stellar mass M_*: $n(> M_{\text{peak}}) > n(> M_*)$ that preserves the rank ordering. In practice, we apply a 0.2 dex log-normal scatter in M at fixed M_{peak} based on observations of the stellar mass to halo mass relation (SMHMR; **bunch of SMHMR citations**). Gu et al. (2016) compile empirical constraints on the scatter of this stellar mass to halo mass relation ($\sigma_{\log M_*}$). Using the SHAM mapping, we can assign galaxy stellar mass to subhalos based on observed stellar mass functions (SMFs) at the redshifts of the simulation outputs (snapshots).

We use the SMF from Li & White (2009) at $z = 0.05$ and at higher redshifts interpolate between the Li & White (2009) SMF and the SMF from Marchesini et al. (2009) at $z = 1.6$. We choose the Li & White (2009) SMF because it is based on the same SDSS NYU-VAGC sample as our SDSS DR7 group catalog (Section 2). We choose the Marchesini et al. (2009) SMF, amongst others, because it produces interpolated SMFs that monotonically increase at $z < 1$. As noted in Hahn et al. (2017a), at $z \approx 1$, the SMF interpolated between the Li & White (2009) and Marchesini et al. (2009) SMFs is consistent with more recent measurements from Muzzin et al. (2013) and Ilbert et al. (2013). At each snapshot, we independently use SHAM to assign galaxy M_*. This way, we not only track the evolution of subhalos, but also the the galaxies' M_*. With the 45 snapshots outputs from our simulation, we can in principle track the central galaxies back to $z \sim 10$. However, we restrict ourselves to snapshots at $z \lesssim 1$, where we have the most statistically meaningful observations. We next describe how we select star forming central galaxies in our model and initalize them. **TBD: Perhaps mention in appendix how we test different SMF assumptions**

3.1.   Selecting Star Forming Centrals

In our model, we're interested in tracking the SFR and stellar mass evolution of SF central galaxies. To construct such a model, we first need to select SF galaxies from the central galaxies in our simulation, described above. Since we want our model to reproduce observations, our selection is based on $f_{\rm SFS}^{\rm cen}(M_*)$, the fraction of central galaxies within the star forming sequence, measured from the SDSS DR7 VAGC (Section 2). Below, we describe how we derive this $f_{\rm SFMS}^{\rm cen}(M_*)$ and use it to select SF central galaxies in our model. Afterwards we describe how we initalize the SFRs and M_* of these galaxies in our model.

Often in the literature, an empirical color-color or SFR-M_* cut that separates the two main modes (red/blue or star-forming/quiescent) in the distribution is chosen to classify galaxies (*e.g.* Baldry et al. 2006; Blanton & Moustakas 2009; Drory et al. 2009; Peng et al. 2010; Moustakas et al. 2013; Hahn et al. 2015). The red/quiescent or blue/star-forming fractions derived from this sort of classification, by construction, depend on the choice of cut and neglect galaxy subpopulations such as transitioning galaxies *i.e.* galaxies in the "green valley". For our $f_{\rm SFMS}^{\rm cen}(M_*)$, we instead use a method from Hahn et al. (in prep) and Tjitske et al. (in prep), which is a data-driven fitting of the SFS from the SFR-M_* distribution using Gaussian Mixture Models (GMMs).

shorten: emphasize the advantages Using the Hahn et al. (in prep) SFS fitting, we fit the SSFR distributions of the SDSS DR7 VAGC centrals in log M_* bins of width 0.2 dex using GMMs with $k = 1 - 3$ components using the expectation-maximization algorithm (EM; Dempster et al. 1977; Neal & Hinton 1998). We restrict ourselves to models with a maximum of 3 components for the three possible galaxy classifications: quiescent, SF, and transitioning populations. From the three GMMs, we select the model with the lowest

Bayesian Information Criteria (BIC; Schwarz 1978). The Gaussian component of this GMM with mean $\log \mathrm{SSFR} > -11$ is identified as the SFMS. In the rare cases when more than one GMM component has mean $\log \mathrm{SSFR} > -11$, we compare the weights of the components. If the weight of one component is less than a third of the other, we take the component with the higher weight to represent the SFMS. Otherwise, we omit the stellar mass bin altogether. **sentence about how for the VAGC, we don't omit any stellar mass bins** The weight of the SFMS GMM component provides an estimate of $f_{\mathrm{SFMS}}^{\mathrm{cen}}$ for the given stellar mass bin. In the right panel of Figure 1, we plot the SFMS GMM component (blue shaded region) of the $p(\log \mathrm{SSFR})$ for the SDSS DR7 central galaxies within $10.6 < \log M_* < 10.8$. The SFMS constitutes $f_{\mathrm{SFMS}}^{\mathrm{cen}} = 0.21$ of the SDSS central galaxies in this stellar mass bin.

Next, using the $f_{\mathrm{SFMS}}^{\mathrm{cen}}$ spanning the different stellar mass bins, we fit $f_{\mathrm{SFMS}}^{\mathrm{cen}}$ as a function of $\log M_*$. Using a fiducial stellar mass of $\log M_{\mathrm{fid}} = 10.5$, we derive the following best-fit

$$f_{\mathrm{SFMS,bestfit}}^{\mathrm{cen}}(M_*) = -0.627 \, (\log \, M_* - 10.5) + 0.354. \tag{1}$$

We note that this $f_{\mathrm{SFMS,bestfit}}^{\mathrm{cen}}(M_*)$ is in good agreement with the $f_{\mathrm{Q}}^{\mathrm{cen}}(M_*; z \sim 0)$ fit from Hahn et al. (2017a). For each central galaxy in our simulation, we assign a probability of it being on the SFMS, using $f_{\mathrm{SFMS,bestfit}}^{\mathrm{cen}}(M_*)$ with M_* at $z \sim 0$ assigned through SHAM. Based on these probablities, we randomly identify central galaxies from our simulation as star-forming at $z \sim 0$.

At this point, to initialize our SF centrals, we make the assumption that once a SF galaxy quenches its star formation, it remains quiescent. **maybe something about rejuvenation?** Without any quenched galaxies rejuvenating their star formation, the central galaxies that we place on the SFMS at $z \sim 0$ were also on the SFMS at $z \sim 1$ — the initial redshift of our model. At $z \sim 1$, we initialize the SF centrals with SHAM M_*s and assign their initial SFRs based on the observed SFR-M_* relation of the SFMS. Observations in the literature at these redshifts, however, not only use galaxy properties derived differently from the SDSS VAGC but they also find SFMS with significant discrepancies from one another. In Speagle et al. (2014), they compile the SFR-M_* relation of the SFMS from 25 studies in the literature, each with different methods of deriving galaxy properties. Even after the calibration, for a fixed $M_* = 10^{10.5} \, M_\odot$, the SFRs of the SFMS from different analyses at $z \sim 1$ vary by more than a factor of 2 (see Figure 2 of Speagle et al. 2014). This is particularly concerning since the redshift evolution of the SFMS dictate the SFR and M_* evolution of SF centrals in our model. So to deal with this uncertainty, we parameterize the SFMS SFR ($\log \mathrm{SFR}_{\mathrm{MS}}(M_*, z)$) with free parameters that characterize the redshift dependence and marginalize over them later in the analysis.

For our $\log \mathrm{SFR}_{\mathrm{MS}}(M_*, z)$, at $z \sim 0$ we anchor our SFMS to the SFMS of the SDSS central galaxies, which we obtain from the SFMS GMM components used to estimate $f_{\mathrm{SFMS}}^{\mathrm{cen}}$. Using the mean $\log \mathrm{SFR}$ of the SFMS GMM component at each stellar mass bin, we linearly fit $\log \mathrm{SFR}(M_*)$ (see dashed line in Figure 1). Then for $z > 0$, we include two free parameters to

account for the redshift evolution of the amplitude and slope of the SFMS SFR-M_* relation: A_z and m_z, respectively. We parameterize the mean log SFR of the SFMS as,

$$\log \overline{\mathrm{SFR}}_{\mathrm{MS}}(M_*, z) = . \tag{2}$$

Then we initialize the $z \sim 1$ SFRs of our SF centrals by randomly sampling a log-normal distribution centered about $\log \overline{\mathrm{SFR}}_{\mathrm{MS}}(M_*, z = 1)$ with a constant scatter of 0.3 dex, motivated from observations (Noeske et al. 2007; **?**; **?**; **?**). Later in our analysis, when we choose priors for A_z and m_z, we conservatively choose a range that encompass the best-fit SFMS from Speagle et al. (2014) and measurements from Moustakas et al. (2013) and Lee et al. (2015). With our SF centrals initalized at $z \sim 1$, next, we describe how we evolve their SFR and M_* in our model.

3.2. Evolving along the Main Sequence

The tight correlation between the SFRs and stellar masses of star-forming galaxies (the so-called SFMS) spans over four orders of magnitude in stellar mass and extends beyond the local universe out to $z > 2$ (*e.g.* Noeske et al. 2007; **?**; **?**; Salim et al. 2007; **?**; **?**; **?**; Moustakas et al. 2013; Lee et al. 2015; see also references in Speagle et al. 2014). In bins of $\log M_*$, the SFRs of galaxies on the SFMS are observed to follow a log-normal distribution with a roughly constant scatter of 0.3 dex. Given its persistence for star-forming galaxies in the local Universe, the SFMS provides a straightforward relationship to characterize the SFRs and M_*s of star-forming galaxies throughout $z < 1$. More specifically, we can characterize the star formation histories (SFHs) of our star-forming centrals with respect to the mean log SFR of the SFMS (Eq. 2):

$$\log \mathrm{SFR}(M_*, t) = \log \overline{\mathrm{SFR}}_{\mathrm{MS}}(M_*, t) + \Delta \log \mathrm{SFR}(t). \tag{3}$$

Since SFH determines the M_* growth of a galaxy, in our model, $\Delta \log \mathrm{SFR}$ dictates both the SFHs and M_* evolution of the star-forming centrals in our model. Below, we describe our specific prescription for $\Delta \log \mathrm{SFR}(t)$.

In the previous section, we selected the initial SFRs of our star-forming centrals by sampling the log-normal distribution about the mean SFMS at $z \sim 1$. One naive prescription for $\Delta \log \mathrm{SFR}(t)$, would be to fix $\Delta \log \mathrm{SFR}$ based on the initial offsets from the $\log \overline{\mathrm{SFR}}_{\mathrm{MS}}$. SF centrals with higher than average initial SFRs continue evolving above the average SFMS, while SF centrals with lower than average initial SFRs continue evolving below the average SFRs. With such SFHs, as we demonstrate later in detail, the scatter in stellar mass of the SF centrals at fixed halo mass diverges substantially with cosmic time. Furthermore, when we examine the SFHs of star-forming galaxies of the Illustris simulation **??**, we find little motivation for constant $\Delta \log \mathrm{SFR}(t)$. In Figure 2, we present $\Delta \log \mathrm{SFR}$ of star-forming
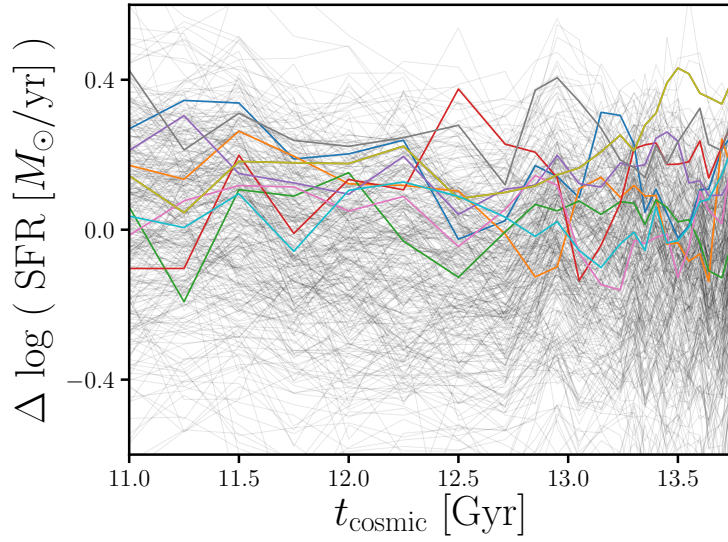
Fig. 2.— Star formation rate with respect to the $\log \overline{\mathrm{SFR}}_{\mathrm{MS}}$ ($\Delta \log \mathrm{SFR}$) as a function of cosmic time for star-forming galaxies in the Illustris simulation. These galaxies have stellar masses within the range $10^{10.5} - 10^{10.6} M_\odot$ at $z \sim 0$. $\log \overline{\mathrm{SFR}}_{\mathrm{MS}}$ is fit using the same as the SFMS fits for the SDSS centrals in Section 3.1. The $\Delta \log \mathrm{SFR}(t)$ of these Illustris star-forming galaxies stochastically fluctuate about the mean SFMS. Our prescription for the SFHs of the SF centrals in our model (Section 3.2) is based on this $\Delta \log \mathrm{SFR}(t)$ behavior.
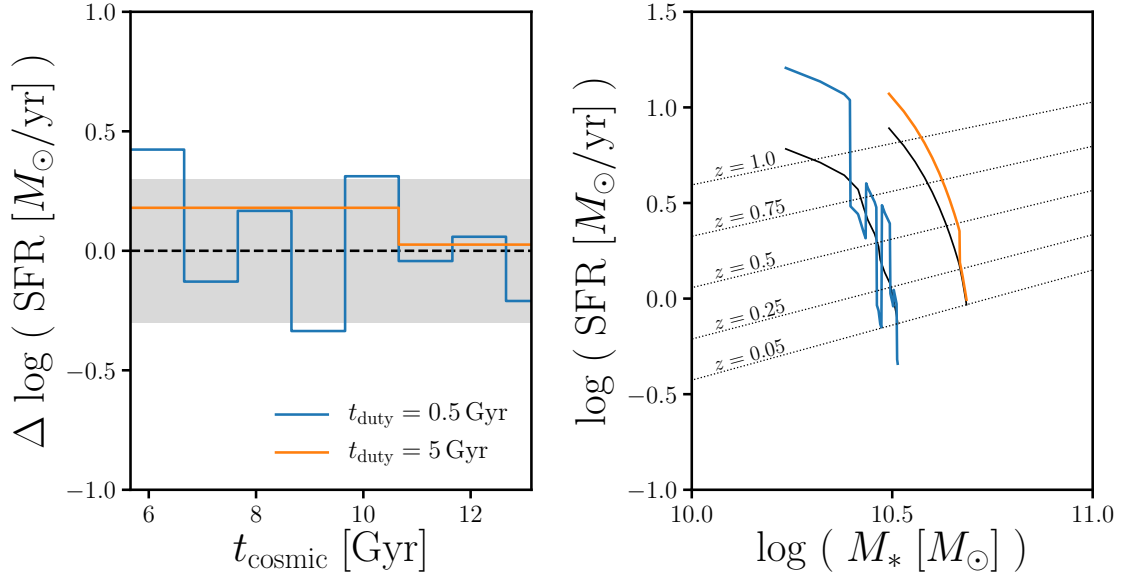
Fig. 3.— *Left*: We illustrate the star formation duty cycle prescription for $\Delta \log \mathrm{SFR}(t)$, described in Section 3.2. The two examples we present have $t_{\mathrm{duty}} = 0.5$ Gyr (blue) and 5 Gyr (orange). The star formation duty cycle $\Delta \log \mathrm{SFR}(t)$ combined with Eq. 3, describe the SFHs of the star-forming central galaxies in our model. *Right*: We present the SFR and M_* evolutions of two SF central galaxies in our model with $t_{\mathrm{duty}} = 0.5$ Gyr (blue) and 5 Gyr (orange). The $\Delta \log \mathrm{SFR}(t)$ for these galaxies correspond to the left panel and can be seen with respect to the $\log \overline{\mathrm{SFR}}_{\mathrm{MS}}(M_*, t)$ plotted in black. For reference, we include the $\log \overline{\mathrm{SFR}}_{\mathrm{MS}}(M_*)$ (dotted lines) at various redshifts between $z = 1$ to 0.05.
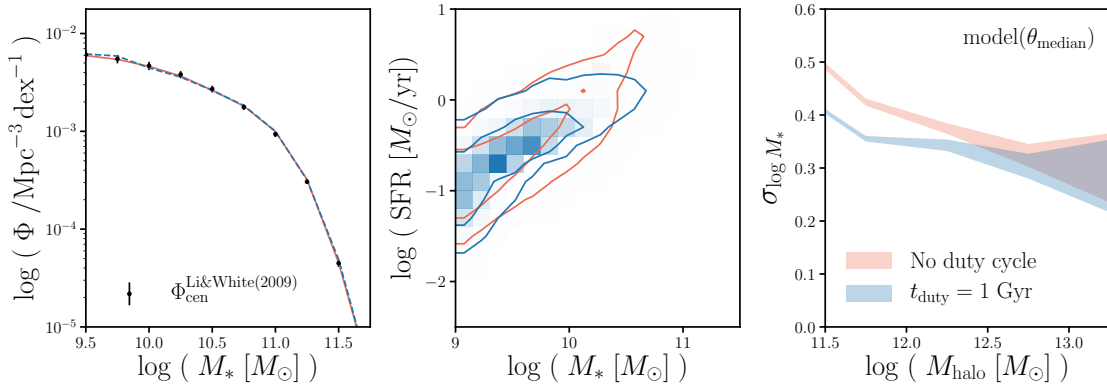

Fig. 4.—

Illustris galaxies as a function of cosmic time. These galaxies have stellar masses within $10^{10.5} - 10^{10.6} M_\odot$ at $z = 0$. At the simultation outputs, we derive $\log \overline{\text{SFR}}_{\text{MS}}$ using the same fitting method we used for the SDSS centrals in Section 3.1 and use it to calculate $\Delta \log \text{SFR}$ (Eq. 3). Rather than remaining constant, Figure 2 illustrates that the $\Delta \log \text{SFR}(t)$s stochastically vary about SFMS.

Motivated by the $\Delta \log \text{SFR}(t)$ of Illustris galaxies, we introduce the "*star formation duty cycle*" to our $\Delta \log \text{SFR}(t)$. We parameterize $\Delta \log \text{SFR}$ to randomly flucutate about the mean SFMS on some duty cycle timescale t_{duty}. Then the SFR of a given SF central in our model will follow Eq. 3 where at every timestep t_{duty}, $\Delta \log \text{SFR}$ is randomly sampled from a log-normal distribution with 0.3 dex scatter. In the left panel of Figure 3, we present $\Delta \log \text{SFR}(t)$ of SF centrals in our model with our star formation duty cycle prescription. The two $\Delta \log \text{SFR}(t)$s have $t_{\text{duty}} = 0.5$ Gyr (blue) and 5 Gyr (orange). The shaded region represents the observed 0.3 dex 1σ scatter of the SFMS SFR. **Such a simplified model obviously does not reflect individual SFHs of SF galaxies; however, since $\Delta \log \text{SFR}$ is randomly sampled, we expect it capture the stochasticity from gas accretion and star-bursts.** Furthermore, this prescription of $\Delta \log \text{SFR}$ produces SFHs that reproduce the log-normal SFR distribution of the SFMS at any point in the model.

Using our $\Delta \log \text{SFR}$ prescription, we now evolve both the SFR and M_* of our SF centrals along the main sequence. Based on Eq. 3, the SFRs of our SF centrals are functions of M_*. Meanwhile, M_* is the integral of the SFR over time:

$$M_*(t) = f_{\text{retain}} \int_{t_0}^{t} \text{SFR}(M_*, t) \, dt + M_0. \tag{4}$$

f_{retain} here is the fraction of stellar mass that is retained after supernovae and stellar winds; we use $f_{\text{retain}} = 0.6$ (Wetzel et al. 2013). t_0 and M_0 are the initial cosmic time and stellar mass at $z \sim 1$, respectively. Combining Eqs. 3 and 4, we get a different equation, which we solve to evolve the SFR and M_* of our SF centrals. The right panel of Figure 3 presents the SFR and M_* evolutions for the two SF centrals with different t_{duty} from the left panel. The behavior of the star formation duty cycle $\Delta \log \text{SFR}(t)$ is clearly evident with respect to $\log \overline{\text{SFR}}_{\text{MS}}(M_*, t)$ (black solid). For reference, we include the $\log \overline{\text{SFR}}_{\text{MS}}$ (dotted lines) at various redshifts between $z = 1$ to 0.05.

Now that we have a model that evolves the SFRs and M_*s of SF centrals, we can compare this model to observations. Our model is constructed using the SMF and SMHMR at $z = 1$ and based on the observed evolution of the SFMS. It has two free parameters A_z and m_z, which allow for a flexible redshift dependence of the SFMS. At the final snapshot, $z \sim 0$, our model reproduces the observed SFR distribution by construction. However, we also want our model to reproduce the observed SMF of central galaxies in SDSS. In order to do a principled comparison of our model to observation, we use the parameter estimation framework of Ap-

proximate Bayesian Computation (ABC). ABC has the advantage over standard approaches to parameter inference in that it does not require evaluating the likelihood. It relies only on a simulation of the observed data and a distance metric to quantify the "closeness" between the observed data and simulation. Many variations of ABC has been used in astronomy and cosmology (*e.g.* ???Alsing et al. 2018). We use ABC in conjunction with the efficient Population Monte Carlo (PMC) importance sampling as in (??). For the priors of A_z and m_z, we use uniform distributions spanning the ranges **numbers** and **numbers**, respectively. As we mentioned in Section 3.1, the range of the prior were conservatively chosen to encompass the best-fit SFMS from Speagle et al. (2014) and measurements from Moustakas et al. (2013) and Lee et al. (2015) at $z \sim 1$. Finally, to compare the SMF of our model to the SMF of SDSS central galaxies, we use the following distance metric:

$$\rho_\Phi = \sum_M \left(\frac{\Phi^{\mathrm{sim}}(M) - f^{\mathrm{cen}}(M)\Phi^{\mathrm{SDSS}}(M)}{\sigma_\Phi(M)} \right)^2. \tag{5}$$

$\Phi^{\mathrm{sim}}(M)$ is the SMF of our model, $f^{\mathrm{cen}}(M)$ is the central galaxy fraction Wetzel et al. (2013), $\Phi^{\mathrm{SDSS}}(M)$ is the Li & White (2009) SDSS DR7 SMF, and $\sigma_\Phi(M)$ is the SMF uncertainty derived using mock catalogs from Li & White (2009). For the rest of our ABC-PMC implementation, we strictly follow the implementation of Hahn et al. (2017b) and Hahn et al. (2017a). We refer reader to those papers for further details.

In Figure 6, we present the SMFs (left), SFMSs (center), and $\sigma_{\log M_*}(\log M_{\mathrm{halo}})$ (right) of the resulting ABC posterior distributions of A_z and m_z for two models with different SFH prescriptions: one with no star formation duty cycle (red) and the other with star formation duty cycle $t_{\mathrm{duty}} = 1\,\mathrm{Gyr}$ (blue). On the left, we illustrate that the ABC posteriors successfully reproduce the $z \sim 0$ SMF of SDSS centrals. In the center, we demonstrate how our models by construction, reproduce the $z \sim 0$ SFMS. Lastly, on the right, we demonstrate that different prescriptions for SFHs in our model produce significantly different scatter in $\log M_*$ for a given $\log M_{\mathrm{halo}}$ — *i.e.* scatter in the SMHMR. Since there are observation constraints on the SMHMR, this means that we can them to better understand and constrain the SFHs of star forming galaxies.

4.   Results

4.1.   The Star Formation Duty Cycle

Our model, described in the previous section, tracks the SFR and M_* evolutions of SF central galaxies. After using ABC,

In the previous section we describe our model constructed from blah with different prescriptions for the star formation histories of star-forming galaxies. As the right panel of Figure 6 demonstrates, different prescriptions for the star-forming galaxy star formation

predicts different $\sigma_{\log M_*}$

- Explain how the posteriors from ABC ultimately marginalize over the parameters that incorporate the uncertainty in the SFMS

- As Figure 6 already demonstrates, different prescriptions lead to different scatter in the SMHMR.

- No duty cycle model obviously ruled out

- In Figure 5 we present the scatter in $\sigma_{\log M_*}$

- We find that by decreasing the timescale of stochasticity on a simple SFH model that traces the overall SFMS evolution does in fact decrease the scatter seen in the SMHMR. However, even with timescales less than XXXX, we cannot reproduce observations. Ultimately to reproduce observations, we need to add in assembly bias.

Figure 5

4.2. The need for a galaxy assembly bias

- discuss how t_{duty} is not enough to be consistent with σ_{M_*}.

- first clarify what you mean by galaxy assembly bias

- discuss implementation of galaxy assembly bias

- Figure (pedagogical) of dlogSFR versus dMh dt for different correlation amounts

- Figure of different tdelay and dtabias

- Figure of sigma M star as a function of duty cycle and realistic dt abias and t delay

5. Discussion

5.1. Rethinking the Main Sequence?
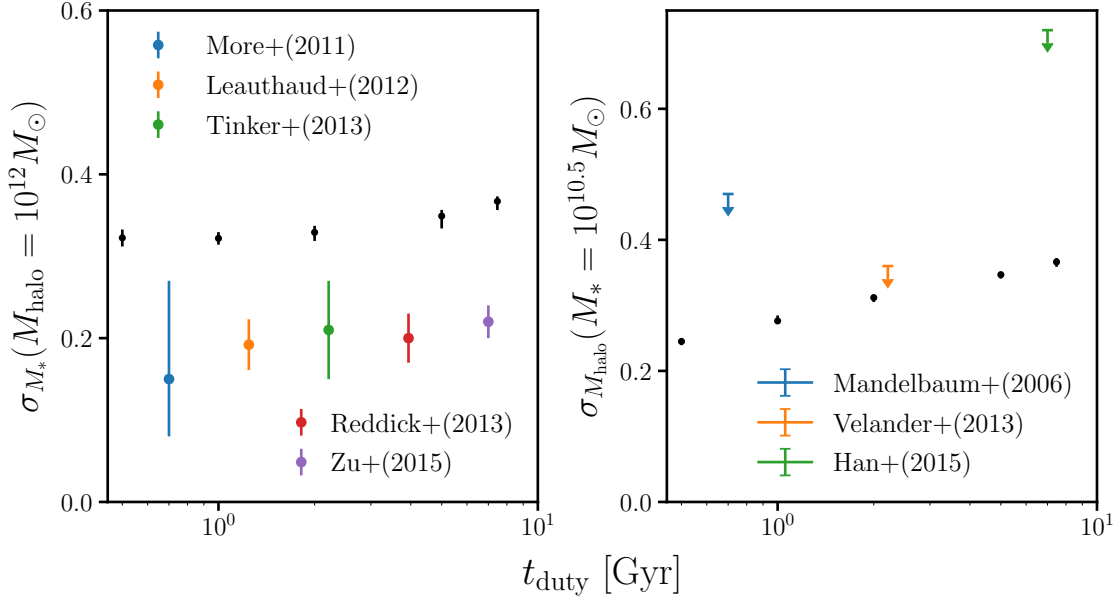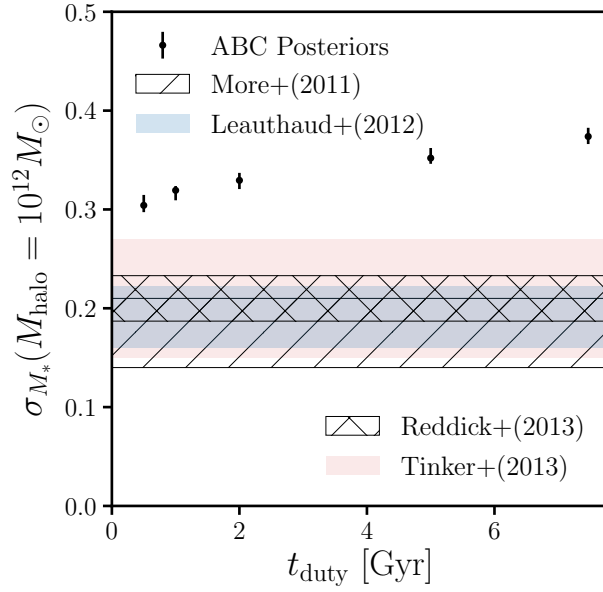
- Test the SMHMR for Louis's SFHs

Fig. 5.—

Fig. 6.—

6. Summary

A. $z \sim 1$ observations

Much of the results presented in this paper are based on comparison between our model and observations at $z \sim 0$.. Our model is initalized at $z \sim 1$. Therefore, in this section we test some of the choices we make in our intializations.

- Test impact of $z \sim 1$ SMF

- Test impact of $z \sim 1$ $\sigma_{\log M_*}$

Acknowledgements

REFERENCES

Abazajian, K. N., Adelman-McCarthy, J. K., Agüeros, M. A., et al. 2009, The Astrophysical Journal Supplement Series, 182, 543

Alsing, J., Wandelt, B., & Feeney, S. 2018, arXiv:1801.01497 [astro-ph], arXiv:1801.01497 [astro-ph]

Baldry, I. K., Balogh, M. L., Bower, R. G., et al. 2006, Monthly Notices of the Royal Astronomical Society, 373, 469

Blanton, M. R., & Moustakas, J. 2009, Annual Review of Astronomy and Astrophysics, 47, 159

Blanton, M. R., & Roweis, S. 2007, The Astronomical Journal, 133, 734

Blanton, M. R., Schlegel, D. J., Strauss, M. A., et al. 2005, The Astronomical Journal, 129, 2562

Brinchmann, J., Charlot, S., White, S. D. M., et al. 2004, Monthly Notices of the Royal Astronomical Society, 351, 1151

Campbell, D., van den Bosch, F. C., Hearin, A., et al. 2015, Monthly Notices of the Royal Astronomical Society, 452, 444

Chabrier, G. 2003, Publications of the Astronomical Society of the Pacific, 115, 763

Conroy, C., Wechsler, R. H., & Kravtsov, A. V. 2006, The Astrophysical Journal, 647, 201

Davis, M., Efstathiou, G., Frenk, C. S., & White, S. D. M. 1985, The Astrophysical Journal, 292, 371

Dempster, A. P., Laird, N. M., & Rubin, D. B. 1977, Journal of the Royal Statistical Society. Series B (Methodological), 39, 1

Drory, N., Bundy, K., Leauthaud, A., et al. 2009, The Astrophysical Journal, 707, 1595

Gu, M., Conroy, C., & Behroozi, P. 2016, The Astrophysical Journal, 833, 2

Hahn, C., Tinker, J. L., & Wetzel, A. R. 2017a, The Astrophysical Journal, 841, 6

Hahn, C., Vakili, M., Walsh, K., et al. 2017b, Monthly Notices of the Royal Astronomical Society, 469, 2791

Hahn, C., Blanton, M. R., Moustakas, J., et al. 2015, The Astrophysical Journal, 806, 162

Ilbert, O., McCracken, H. J., Le Fèvre, O., et al. 2013, Astronomy and Astrophysics, 556, A55

Lee, N., Sanders, D. B., Casey, C. M., et al. 2015, The Astrophysical Journal, 801, 80

Leja, J., van Dokkum, P., & Franx, M. 2013, The Astrophysical Journal, 766

Li, C., & White, S. D. M. 2009, Monthly Notices of the Royal Astronomical Society, 398, 2177

Marchesini, D., van Dokkum, P. G., Förster Schreiber, N. M., et al. 2009, The Astrophysical Journal, 701, 1765

Moustakas, J., Coil, A. L., Aird, J., et al. 2013, The Astrophysical Journal, 767, 50

Muzzin, A., Marchesini, D., Stefanon, M., et al. 2013, The Astrophysical Journal, 777, 18

Neal, R. M., & Hinton, G. E. 1998, in Learning in Graphical Models, NATO ASI Series (Springer, Dordrecht), 355

Noeske, K. G., Weiner, B. J., Faber, S. M., et al. 2007, The Astrophysical Journal Letters, 660, L43

Peng, Y.-j., Lilly, S. J., Kovač, K., et al. 2010, The Astrophysical Journal, 721, 193

Salim, S., Rich, R. M., Charlot, S., et al. 2007, The Astrophysical Journal Supplement Series, 173, 267

Schwarz, G. 1978, The Annals of Statistics, 6, 461

Speagle, J. S., Steinhardt, C. L., Capak, P. L., & Silverman, J. D. 2014, The Astrophysical Journal Supplement Series, 214, 15

Tinker, J., Wetzel, A., & Conroy, C. 2011, ArXiv e-prints, 1107, arXiv:1107.5046

Tinker, J. L., Hahn, C., Mao, Y.-Y., & Wetzel, A. R. 2017, arXiv:1705.08458 [astro-ph], arXiv:1705.08458 [astro-ph]

Vale, A., & Ostriker, J. P. 2006, Monthly Notices of the Royal Astronomical Society, 371, 1173

Wetzel, A. R., Cohn, J. D., & White, M. 2009, Monthly Notices of the Royal Astronomical Society, 395, 1376

Wetzel, A. R., Tinker, J. L., & Conroy, C. 2012, Monthly Notices of the Royal Astronomical Society, 424, 232

Wetzel, A. R., Tinker, J. L., Conroy, C., & van den Bosch, F. C. 2013, Monthly Notices of the Royal Astronomical Society, 432, 336

—. 2014, Monthly Notices of the Royal Astronomical Society, 439, 2687

Wetzel, A. R., & White, M. 2010, Monthly Notices of the Royal Astronomical Society, 403,

1072

White, M. 2002, The Astrophysical Journal Supplement Series, 143, 241

White, M., Cohn, J. D., & Smit, R. 2010, Monthly Notices of the Royal Astronomical Society, 408, 1818

Yang, X., Mo, H. J., & van den Bosch, F. C. 2009, The Astrophysical Journal, 695, 900

Yang, X., Mo, H. J., van den Bosch, F. C., & Jing, Y. P. 2005, Monthly Notices of the Royal Astronomical Society, 356, 1293